

Characterization of the beryllium substitutional pair in silicon by infrared spectroscopy

J. N. Heyman and E. E. Haller

*University of California at Berkeley, Berkeley, California 94720
and Lawrence Berkeley Laboratory, Berkeley, California 94720*

A. Giesekeus

Institut für Physik, Universität Dortmund, D-4600 Dortmund, Germany

(Received 30 May 1991; revised manuscript received 19 August 1991)

We have performed a detailed, high-resolution infrared study of a beryllium-related center in silicon with ionization energy $E_0 + 145.8$ meV. Very-high-signal-to-noise-ratio transmission spectra have been obtained that show qualitatively different features. The excitation spectrum of this center, which we designate as Be_2 , consists of an acceptor-effective-mass line series accompanied by a second weaker series displaced to higher energy by 2 meV. We present absorption spectra obtained under uniaxial stress. The stress data show that the center possesses trigonal point symmetry, and indicate that the two series arise from one defect. We develop a simple model of a neutral, trigonal double acceptor in which the hole-hole correlation effects are included in the description of the ground state, but are neglected in the treatment of the effective-mass-like excited states. This model explains our experimental results. We suggest that the center is a beryllium pair in which Be atoms occupy nearest-neighbor Si sites. Recent calculations indicate that the substitutional pair should be metastable under certain conditions, and that the lowest-energy configuration of this center should be a double acceptor.

I. INTRODUCTION

Doping silicon with beryllium introduces several defects. Line spectra of four acceptor centers¹⁻⁴ with ionization energies 191.9, 145.8, 198, and 103.5 meV have been identified by infrared spectroscopy. In addition, a Be-H and two Be-Li centers have been discovered.^{1,5} The Be-H and Be-D centers have been studied extensively,^{6,7} and have been shown to be tunneling hydrogen centers. One Be-Li center has been shown⁷ to be a static center. Samples may be prepared in which more than 90% of the beryllium is electrically inactive. An isoelectronic defect has been studied by photoluminescence and Raman techniques.^{8,9}

Divalent beryllium should capture two electrons to occupy the substitutional site, and should form a double acceptor. It has been suggested that the 191.9-meV level (Be_1) is due to isolated substitutional Be. A recent piezospectroscopic study³ indicates that the center is a tetrahedral double acceptor, supporting this suggestion. Annealing studies show that the concentration of the 145.8-meV level is increased by slow cooling from $T > 600^\circ\text{C}$, but is reduced by a rapid quench. On this basis, Crouch and Robertson infer that this level is due to a complex. They suggest a model consisting of beryllium atoms on nearest-neighbor substitutional sites. Calculations¹⁰ predict that the lowest-energy configuration of such a center has a broken bond between the two beryllium atoms, which then relax towards the plane of the neighboring silicon atoms, and is a double acceptor.

It is possible to identify double acceptors with infrared spectroscopy in both neutral and singly ionized charge states. The singly ionized center is characterized by a

$Z = 2$ Rydberg series. In the neutral species, Coulomb and exchange interactions between the two bound holes may cause splittings of the ground and excited states relative to the single-acceptor excitation spectrum.¹¹⁻¹³ In addition, uniaxial stress techniques give the symmetry properties of the double-acceptor eigenfunctions, which differ from those of simple acceptors. Double acceptors have been studied in both charge states in germanium.^{14,15} In silicon, in addition to the 191.9-meV center, splittings of the ground and excited states have been observed^{16,17} in the ir spectrum of Si:Zn.

In this paper we show that it is also possible to characterize nontetrahedral neutral double acceptors with ir spectroscopy. We use ir spectroscopy combined with uniaxial stress to identify a trigonal double acceptor, which we believe is the beryllium substitutional pair.

II. EXPERIMENTAL PROCEDURE

Bulk beryllium-doped silicon was obtained by high-temperature diffusion. Approximately 1000 Å of 99.9% pure beryllium metal were evaporated onto greater than 1000 Ωcm p -type or 70 Ωcm n -type high-purity floating-zone silicon. Samples were sealed into quartz ampoules with an ambient of helium. Diffusion took place at 1300°C for 30–45 min, after which the samples were removed from the furnace. The cooling rate was measured to be approximately 300°C/min. Secondary-ion-mass-spectroscopy (SIMS) and resistivity measurements performed on selected samples measured a beryllium concentration of $(1-5) \times 10^{16} \text{ cm}^{-3}$ and room-temperature hole concentrations of 10^{14} cm^{-3} to $5 \times 10^{16} \text{ cm}^{-3}$. Transmission samples were typically $1 \times 1 \times 0.1$

cm^3 . Samples for uniaxial stress measurements were oriented to within 1° by Laue x-ray diffraction. Stress samples were cut to $1 \times 0.4 \times 0.2 \text{ cm}^3$ with the 1-cm axis along either the $\langle 111 \rangle$ or $\langle 100 \rangle$ direction.

Infrared transmission spectra were obtained with a Digilab 80E-V Fourier-transform spectrometer. For these measurements samples were mounted in a Janis Super-VP exchange gas optical cryostat. Transmitted light was concentrated either onto a Ge:Cu photoconductor mounted in our cryostat, or onto an external TGS pyroelectric detector. Transmission was measured over the range $450\text{--}4000 \text{ cm}^{-1}$. Instrumental spectral resolution was typically set at 0.5 cm^{-1} .

Transmission measurements under uniaxial stress were performed in a stress cell that may be mounted in our optical cryostat. The construction is similar to cells used by others.¹⁸ The sample is placed between two pistons. Force is applied to the upper piston through a push rod from outside the cryostat. A known force is generated by a gas piston at room temperature. In this system stress may be changed *in situ*.

The homogeneity and reproducibility of the applied stress were tested by uniaxial stress measurements of boron-doped silicon, a system which has been previously characterized.¹⁹ Stress-induced broadening was typically below the zero-stress linewidth of the Be_2 line series. An infrared polarizer was used to measure stress-induced dichroism in this system. The polarizer consists of a wire grid on a KRS5 substrate.

III. EXPERIMENTAL RESULTS

A. ir transmission at zero stress

Infrared spectra of our Si:Be samples show transitions from the $E_v + 191.9\text{-meV}$ acceptor level (Be_1) as well as the $E_v + 145.8\text{-meV}$ acceptor level which we designate Be_2 . In this paper we discuss the Be_2 center exclusively. ir transmission measurements at 5 K show a series of absorption lines in the region $130\text{--}150 \text{ meV}$ (Fig. 1). The spacing and relative intensity of five strong lines is consistent with transitions to acceptor Rydberg states from a ground state at $E_v + 145.8 \text{ meV}$. The spacing and relative intensity of the remaining weaker lines match a second acceptor-effective-mass series. The energy positions are given in Table I. We designate the strong and weak series α and β , respectively. The shift between corresponding lines of the two series varies from $1.9\text{--}2.1 \text{ meV}$. The relative intensities of corresponding lines of the α and β series are approximately 5:1 and are constant in all samples measured. Our data are consistent with previous measurements. All of the lines associated with the Be_2 center may be recognized in the published spectra of Peale, Muro, and Sievers,⁷ although they do not refer to or discuss the β series lines. Only the four strongest lines (Be_2 1α , 2α , 2β , 4α in our notation and Be_{II} 1, 2, 3, 4 in their notation) were observed by Crouch, Robertson, and Gilmer.¹

Two series of broad features are seen in the continuum absorption region of the Be_2 absorption spectrum, shown in Fig. 2. These appear at energies equal to the energies

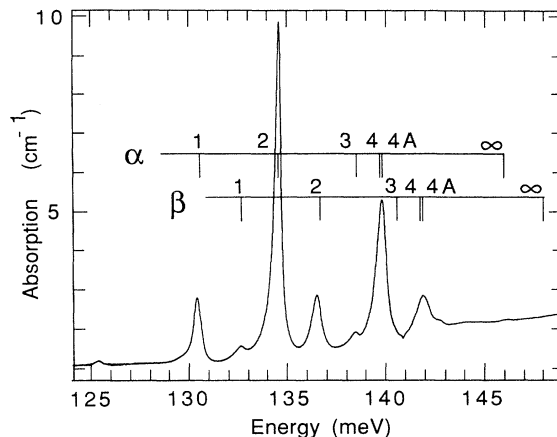


FIG. 1. Sharp line absorption spectrum of the Be_2 center. The markers show the line separations of simple acceptor Rydberg series in silicon. Two overlapping effective-mass series separated by about 2.1 meV are seen. A weak feature at 124.4 meV is not related to the Be_2 center.

of the sharp lines plus 64.4 meV , the energy of the zone-center optical phonon in silicon. Similar features have been observed^{20,21} for many acceptors in silicon, including B, Ga, Al, and In, and are identified as Breit-Wigner-Fano-type resonances of a discrete state with a continuum.^{22,23} They arise from a resonance of virtual bound states, consisting of an electronic excited state plus an optical phonon, with the valence-band states. The intensities of the α and β Fano resonance series are approximately equal.

Transitions to Rydberg states associated with the split-off valence band cannot be measured for either series. These would be obscured by the much stronger absorption lines of the Be_1 series.

Measurements have been made at temperatures between 4 and 50 K. We find the relative intensities of the α and β series to be temperature independent over this range. No new features are seen at higher temperatures. This is in agreement with measurements by Peale, Muro,

TABLE I. Ground- to excited-state spacing for the Be_2 center. Data for B and Al acceptors are included for comparison.

Line No.	Be_2 α	Be_2 β	B ^a	Al ^b
1	130.40	132.61	30.38	54.88
2	134.49	136.46	34.49	58.49
3	138.4		38.35	
4	139.74	141.84	39.57	64.08
4A			39.65	64.96
4B			39.88	65.16

^aReference 25.

^bReference 26.

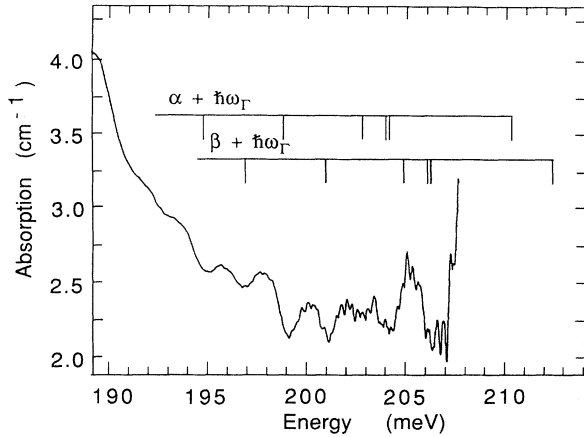


FIG. 2. Breit-Wigner-Fano resonance in the continuum absorption of the Be_2 center. Resonance arise from transitions to the quasibound states which consist of an electronic excitation plus the creation of a zone-center optic phonon. Markers show positions of the Be_2 α and β series plus $\hbar\omega_\Gamma = 64.4$ meV. Strong competing continuum absorption from the Be_1 center degrades the signal to noise above 200 meV.

and Sievers⁷ over the range 1.7–50 K, which also show no new features at elevated temperatures. These results prove that the two series do not arise from a splitting of the ground state of the system. These data also suggest that there is no higher state in the ground-state manifold, which may be significantly populated at $T < 50$ K. To be consistent with our measurements, the nearest level from which transitions may be observed must be at least 5 meV above the ground state.

In addition, a much weaker line is observed at 125.41 meV, which is not correlated with the intensity of the Be_2 series. The temperature dependence of the linewidth and intensity of the 125.41-meV feature are similar to the Be_2 series, indicating that this line also arises from an electronic transition.

B. Uniaxial stress measurements

Transmission measurements have been made of $\langle 111 \rangle$ and $\langle 100 \rangle$ stress in the range 0–150 MPa. The results are summarized in Fig. 3. The well-known splittings of the acceptor-effective-mass excited states are observed in both the α and β series. The relative intensities of the stress-split components are temperature independent. This indicates that the ground state does not split under stress.

The behavior of the acceptor-effective-mass states under uniaxial stress is well understood. The twofold states, which transform like Γ_6 or Γ_7 , shift but do not split. The fourfold Γ_8 states split into two Kramers doublets under any orientation of stress. The final states of lines 1 and 2 of the acceptor-effective-mass series are Γ_8 states. The final states of lines 4 and 4A are, respectively, Γ_6 and Γ_7 states. The splitting of the Γ_8 levels under $\langle 111 \rangle$ and $\langle 100 \rangle$ stress are $\Delta_{\langle 100 \rangle} = 2b(s_{11} - s_{12})T$, and $\Delta_{\langle 111 \rangle}$

$= (d/\sqrt{3})s_{44}T$, where the elements s_{ij} are the elastic compliance constants, T is the applied stress, and b and d are deformation potential constants. The constants b and d are defined for each level, but are typically close to the valence-band values.

All the observed splittings of the α - and β -line series under $\langle 100 \rangle$ stress may be understood on the basis of well-known models of acceptor-effective-mass states under uniaxial stress. The deformation potential b for the final states of lines 1 and 2 may be determined from the line splittings. The values are comparable to deformation potentials obtained from other acceptors¹⁹ and from theory.²² Within experimental error, values of b obtained for the α and β series are equal.

The $\langle 111 \rangle$ stress results may be summarized as follows: Splittings of the lines of the α series are observed

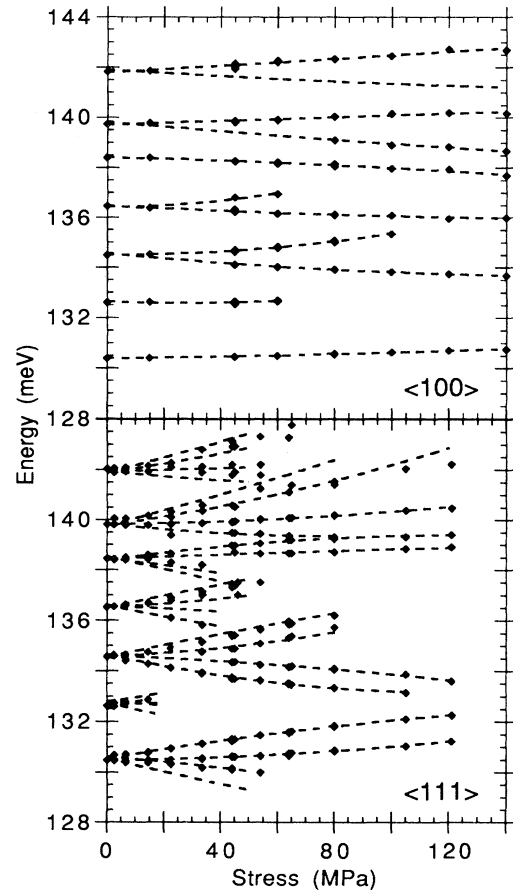


FIG. 3. Peak positions as a function of $\langle 100 \rangle$ and $\langle 111 \rangle$ applied stress. Dashed lines show line splittings predicted by our model. Splittings of weak features such as the β -series lines are not completely resolved in these measurements. Under $\langle 100 \rangle$ stress, the fourfold-degenerate excited state of line 2α splits into two Kramers doublets. The twofold excited states of lines 4 and 4A separate but do not split. Under $\langle 111 \rangle$ stress an additional splitting of these lines is observed due to a lowering of the orientational degeneracy. These results indicate that the Be_2 center is trigonal.

which are qualitatively similar to predicted splittings of acceptor-excited states under $\langle 111 \rangle$ stress.²² Deformation-potential values for the final states of lines 1 and 2 calculated from our data are comparable to values obtained for simple acceptors and to results of theory. However, there is an additional linear splitting of all lines of 27 meV/GPa. An exception to this simple description is seen in line 1, in which only three of the expected four components are seen.

Measurements have been made with light polarized either parallel or perpendicular to the stress axis. Results are shown in Fig. 4. A clear stress-induced dichroism is observed, which is discussed below.

Lines of the β series broaden rapidly with stress, and stress-induced splittings are poorly resolved. However, both the effective-mass-like splitting and the additional splitting of line 2β are seen in certain spectra (Fig. 4). Within the limits of our experiment, the pattern and magnitude of the stress-induced splittings of both series are identical. The deformation-potential values obtained from our data are summarized in Table II.

IV. DISCUSSION

A. Defect symmetry

We have found a splitting of the lines of the Be_2 series under $\langle 111 \rangle$ stress in addition to the splitting of the $2p$ envelope states expected from effective-mass theory. We infer that the Be_2 center is trigonal. In the piezospectroscopy of noncubic centers, orientational splittings may occur. Centers may be distorted along a number of equivalent axes. Uniaxial stress makes one or more of these axes inequivalent to the others. Centers with different orientations shift by different amounts and thus line splittings are observed.

The piezospectroscopy of noncubic centers in cubic crystals has been treated by Kaplyanskii.²³ In the linear approximation, the shift of transition energies is given by

$$\Delta = \sum_{i,j} A_{i,j} \sigma_{i,j}, \quad (1)$$

where $\sigma_{i,j}$ are the elements of the stress tensor. The

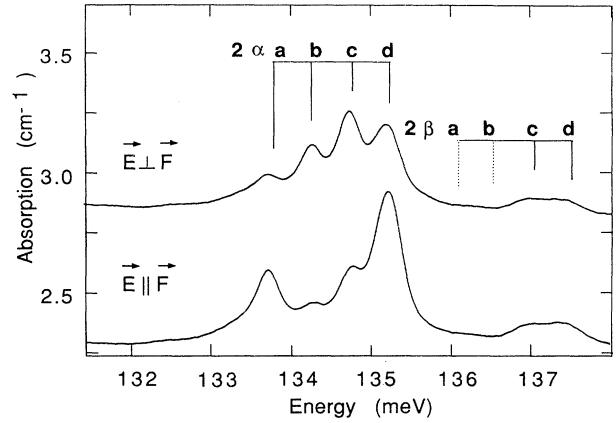


FIG. 4. Lines 2α and 2β at $F \parallel \langle 111 \rangle = 46$ MPa showing stress-induced dichroism. Markers show the fourfold splitting of line 2α and the expected splitting of line 2β . Dotted-line markers indicate predicted features that are not experimentally resolved.

stress tensor is defined by $\sigma_{ij} = n_i n_j T$, where T is the compressional stress and n_i and n_j are direction cosines of T relative to the axis of the center. Thus the elements σ_{ij} are different for centers aligned along different axes. The number of independent coefficients $A_{i,j}$ is determined by the symmetry of the center. For centers with trigonal symmetry the energy shift is determined by just two independent parameters:

$$\Delta = \sum_i A_1 \sigma_{i,i} + 2 \sum_{i < j} A_2 \sigma_{i,j}. \quad (2)$$

Under $\langle 111 \rangle$ stress, centers aligned along the stress axis $[111]$ and those aligned along the three other $\langle 111 \rangle$ directions shift by different amounts, while under $\langle 100 \rangle$ stress all orientations of trigonal centers are equivalent.

$$[111] \text{ stress } \Lambda_{[111]} - \Lambda_{[1\bar{1}\bar{1}]} = \frac{8}{3} A_2, \quad (3)$$

$$[100] \text{ stress } \Lambda_{[111]} - \Lambda_{[1\bar{1}\bar{1}]} = 0. \quad (4)$$

TABLE II. Summary of the uniaxial stress data for the Be_2 center. The constants b , d , A_1 , and A_2 are defined in the text. Deformation-potential constants of B and Al included for comparison. Excited states are labeled by the single-particle notation. The values in parentheses denote the uncertainty in the least significant digit.

	Deformation-potential constants				Piezospectroscopic tensor element	
	b (eV)	d (eV)	A_1	A_2	(meV/GPa)	
	$1\Gamma_{8-}$	$2\Gamma_{8-}$	$1\Gamma_{8-}$	$2\Gamma_{8-}$		
$\text{Be}_2 \alpha$	0.0(1)	0.90(8)	-2.53(30)	1.57(20)	2(2)	10.2(5)
$\text{Be}_2 \beta$	0.0(3)	0.82(15)		1.58(40)	3(5)	13(2)
B^a	0.20(15)	1.61	-2.31(25)	2.64(25)		
Al^a	0.10(5)	1.43	-3.11(22)	2.56(22)		
Theory ^b	-0.025	1.09	-1.84	2.04		

^aReference 19.

^bReference 22.

Therefore, lines will split into two components under $\langle 111 \rangle$ stress, but remain unsplit by $\langle 100 \rangle$ stress. If the well-known splitting of the acceptor-excited states is included, the trigonal model explains all of the stress-induced splittings observed in our data, and we obtain for the Be_2 center

$$A_1 = 2(2) \text{ meV/GPa}, \quad A_2 = 10.2(5) \text{ meV/GPa}.$$

The value of A_2 is obtained from the splitting of $2\alpha a$ and $2\alpha c$ (see Fig. 4). The parameter A_1 describes a shift of all lines. This was obtained from the difference between the shift of line 1α under $\langle 100 \rangle$ stress, and the shift of the $1\Gamma_8^-$ excited state calculated by Buczko.²²

A sample in equilibrium at zero stress will have equal populations of centers aligned along each of the four $\langle 111 \rangle$ axes. If there is no preferential orientation of the centers under $\langle 111 \rangle$ stress, $\frac{1}{4}$ of the centers will be aligned along the stress axis and $\frac{3}{4}$ will be aligned along the other equivalent axes. Stress will then split each line into two components, and the relative intensity under unpolarized light will be 1:3. This simple case is not always realized in real systems. At high stress, mixing between levels may alter the transition probabilities for the two groups of centers. In certain systems, stress-induced reorientation of defects may occur. We find the ratio of intensities of lines ($2\alpha a + 2\alpha b$) to ($2\alpha c + 2\alpha d$) is about 1:2 for $T = 46$ MPa under unpolarized light.

Centers aligned along the stress axis possess C_{3v} sym-

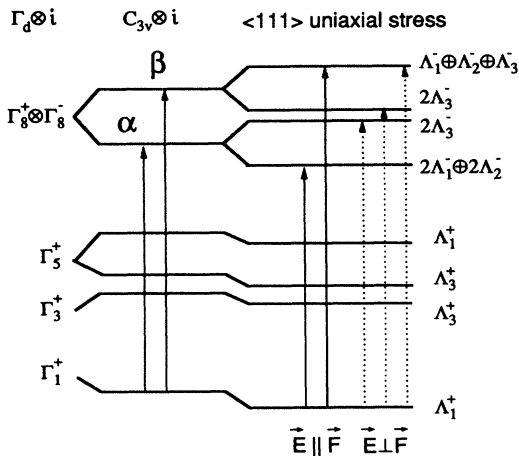


FIG. 5. Proposed level diagram for the Be_2 showing the ground state and line-2 excited state, and allowed electric dipole transitions. Solid vertical lines mark transitions that are allowed for light polarized parallel to the stress axis. Dotted lines mark transitions that are allowed for light polarized perpendicular to the stress. The left-hand side corresponds to the tetrahedral double acceptor. The center shows the influence of a trigonal central-cell distortion. The right-hand side shows the effect of an additional $\langle 111 \rangle$ uniaxial stress. This diagram is only appropriate for the class of centers oriented along the stress axis, e.g., lines $2\alpha a$, $2\alpha b$, $2\beta a$, and $2\beta b$. $\langle 111 \rangle$ stress reduces the symmetry of the remaining centers to the low-symmetry group C_{1h} .

metry. Polarization selection rules for dipole transitions at these centers are shown in Fig. 5. We expect that lines $2\alpha b$ and $2\beta a$ will be absent under light polarized parallel to the stress axis, and $2\alpha a$ will be absent under light polarized perpendicular to the stress axis. Agreement with experiment is reasonable. Because of the fast-concentrating optics used, some depolarization of the beam at the sample surface is expected. The symmetry of centers aligned along the remaining $\langle 111 \rangle$ directions is lowered to C_{1h} by the stress. There are no polarization selection rules from these centers.

B. Origin of α and β series

We have shown that the piezospectroscopic matrix elements of the α and β series are identical. These parameters are probes of the defect microscopic environment, and may serve to label a defect. We have also found that the ratio of intensities of the two series is constant in all samples measured. These data strongly suggest that the α and β series arise from the same center.

Because the relative intensities of the two series is temperature independent, the series must arise from a splitting of the excited states. This splitting reflects an additional degree of freedom of Be_2 relative to simple acceptors. This can be seen by noting the presence of line 4 in both series. In simple acceptor systems, the final state of line 4 is a Kramers doublet, which must remain unsplit in the absence of a magnetic field. Therefore, if Be_2 were a trigonal simple acceptor, line 4 could not appear in both series. In principle this additional excitation may be electronic or vibronic. Phonon sidebands of electronic transitions have been observed²⁴ in the excited-state spectrum of Si:Pt. These sidebands involve the excitation of a pseudolocalized phonon. However, the Be (resonant) vibrational mode² is approximately 63.2 meV. We feel that it is unlikely that vibrational modes of the Be complex could produce the 2-meV excitation observed. We therefore assume an electronic origin for the splitting.

C. Model

Our experimental results may be qualitatively explained by a trigonal double-acceptor model if we make the following reasonable assumptions: First, the effect of the interaction between the two bound holes must be taken into account in a description of the ground state, but may be ignored to first approximation in a description of the excited states. Second, the trigonal distortion of the central cell does not affect bound holes in p -effective mass states. A level scheme suggested by our model is shown in Fig. 5.

The first assumption clearly applies to deep centers because a strong attractive central-cell potential increases the overlap between two holes in a $(1s)^2$ ground-state configuration, whereas the overlap between the holes in a $1s2p$ excited state decreases with increasing depth. The splitting of the double-acceptor $1s2p$ state by the exchange interaction has been treated by Giesekus and Falicov.¹² A reasonable upper boundary of about 0.5 meV is

obtained from a scaling of the triplet-singlet splitting of neutral helium. The splitting may be much smaller in this system due to the central cell potential. The zero-stress linewidth we measure is about 0.38 meV. The unresolved high-energy shoulder of line 1 α may indicate a breakdown of this assumption.

The second assumption is also reasonable. While the central-cell potential strongly perturbs the energies of acceptor and donor ground and even-parity-excited states, the energy of the odd-parity-excited states, which have a *p*-like (or *f*-like) envelope function with vanishing amplitude at the impurity site, is, to good approximation, independent of the central-cell chemistry. The center under investigation is believed to consist of two Be atoms placed on neighboring substitutional sites. In this case, central-cell effects are *not* short ranged, because the total acceptor potential must contain nonzero quadrupole and higher multipole terms. However, we have estimated that the splitting of the *2p* states due to the quadrupole potential will be about 0.04 meV. This is about one order of magnitude smaller than the zero-stress linewidths, and is thus experimentally unresolvable.

We now consider the consequences of the assumptions introduced above for the excited states. In an independent-hole approximation for double-acceptor excited states, the proper symmetry classification for a nondistorted, tetrahedral impurity is given by the irreducible representations of the point group T_d . The wave function of the hole in the *s* state transforms according to Γ_8 , the fourfold-degenerate double-valued representation. The *p*-like states split into two Γ_8 components (lines 1 and 2), a Γ_6 (twofold) and a Γ_7 (twofold) component (lines 4 and 4A). The center studied here has lower symmetry: A trigonally distorted substitutional defect would have site symmetry C_{3v} . If the defect is a nearest-neighbor substitutional pair, the inversion center of the diamond lattice is restored, and the symmetry is the direct product group $C_{3v} \otimes i = D_{3d}$, where the group *i* consists of the unit element and the inversion. The group C_{3v} has three single-valued representations: Λ_1 (one dimensional), Λ_2 (one dimensional), and Λ_3 (twofold). The double-valued representations are Λ_4 (twofold), and a Kramers doublet $\Lambda_{5,6}$. We omit the additional parity quantum number for the representations of D_{3d} , because dipole transitions connect only states of different parity; hence only one of the two sets of states is accessible.

The trigonal symmetry of the center splits the Γ_{8s} state of the *1s2p* excited-state configuration into two doublets, Λ_4 and $\Lambda_{5,6}$. As discussed above, the two Γ_8 *p* states also split because of the trigonal distortion, but the splitting is unresolvable. At zero stress, all the excited states are split because of the *s* state splitting. This explains the appearance of the α and β line series.

External stress further lowers the site symmetry, but the *1s*-like states cannot split further. A twofold degeneracy must remain because of time-reversal symmetry. For the same reason, the Γ_6 and Γ_7 components of the *p* states cannot split, but two components, which are nearly degenerate at zero stress, may separate. The only effect that can appear is the removal of the accidental degeneracy

of the $\Lambda_4 \otimes \Lambda_{5,6}$ quartets that correspond to the *2p*- Γ_8 states of a tetrahedral acceptor. These split into two Kramers doublets under any orientation of stress. As discussed above, the special case of $\langle 111 \rangle$ stress yields an additional splitting due to a lowering of the orientational degeneracy of the trigonal centers.

The ground state of a tetrahedral double acceptor with two noninteracting holes transforms according to the antisymmetric product $\{\Gamma_8 \otimes \Gamma_8\}$. If the hole-hole interaction is ignored, a trigonal distortion will split this ground state into three states: two nondegenerate states $\{\Lambda_4 \otimes \Lambda_4\}$ and $\{\Lambda_{5,6} \otimes \Lambda_{5,6}\}$ and a fourfold state ($\Lambda_4 \otimes \Lambda_{5,6}$). In the nondegenerate states, both holes are in either the lower or higher one-particle states, whereas in the fourfold state, one hole appears in each one-particle state. If this noninteracting picture were accurate, the β series would not appear: the dipole transition is a one-particle *s-p* transition, and the quantum numbers of the remaining *1s* hole remain unchanged; thus the ground state would connect only to the α series. However, the independent hole picture is inappropriate, because a description of the ground-state manifold requires that we consider the Coulomb interaction between the two holes: The $\{\Gamma_8 \otimes \Gamma_8\}$ ground state of a tetrahedral double acceptor with interacting holes splits into three distinct levels: Γ_1 , Γ_3 , and Γ_5 . The magnitude of the level splittings has been calculated¹¹ for double acceptors in silicon. For a physically reasonable choice of parameters, the splitting between the Γ_5 and Γ_3 levels is found to be of order 1 meV. The separation between the Γ_5 and Γ_1 levels is expected to be much larger, of order 40 meV. A trigonal central-cell potential will split the Γ_5 level, leaving a nondegenerate Λ_1 state, two twofold Λ_3 states, and another nondegenerate level that transforms according to Λ_1 . Dipole transitions will connect all of these states to states of the α and β series. We see that transitions to the β series excited states are only allowed by the hole-hole interaction. This description explains why the β series is much weaker than the α series. In the Fano resonance series ordinary selection rules do not apply because of the interaction with the phonon. Here the α and β series have roughly equal strength.

From our stress and temperature data we infer that the ground state of the Be₂ center is a Λ_1 singlet state which is at least 5 meV below the nearest level in the $(1s)^2$ manifold. There are two $(1s)^2\Lambda_1$ levels in our model, one originating from the Γ_1 level, and one originating from the splitting of the Γ_5 level. We tentatively suggest that the ground state of the system is the singlet state arising from the Γ_1 level. The separation between this state and the other $(1s)^2$ states should be large. However, the splitting of the Γ_5 level may be expected to be of the same order as the α - β splitting (2 meV). If the singlet state arising from the Γ_5 level were the ground state, we would expect that the nearest Λ_3 level could be thermally populated, in contradiction to our measurements. Thewalt and co-workers^{14,15} have observed that the ground state of the double acceptors Ge:Zn and Ge:Be is a Γ_1 state. However, the ground state of the Be₁ double acceptor in silicon has been shown³ to be Γ_5 .

V. SUMMARY

We have made a study of the Be-related complex Be_2 using infrared spectroscopy with uniaxial stress. A Fano resonance series and a 2-meV splitting of the excited states is observed. We obtain deformation potentials for the excited states which are comparable to values measured for other acceptors in silicon. Additional splittings may be explained by a trigonal model with piezospectroscopic tensor elements $A_1=2(2)$ meV/GPa and $A_2=10.2(5)$ meV/GPa. A model for a trigonally distorted double acceptor is presented which qualitatively explains our experimental data. Our measurements support the microscopic model for the center of two berylli-

um atoms on nearest-neighbor substitutional sites originally suggested by Crouch, Robertson, and Gilmer¹.

ACKNOWLEDGMENTS

The authors would like to acknowledge the valuable assistance of Professor L. M. Falicov in the interpretation of our data. In addition, we would like to thank W. Hansen, W. Walukiewicz, and E. Merk for their suggestions and guidance. Finally, we wish to thank J. Beeman for constructing our Ge:Cu photoconductor, and J. Walton for the use of his evaporation facilities. This work was supported by NSF Grant No. DMR-88-06756. One of us (A. G.) acknowledges the support of the Deutsche Forschungsgemeinschaft (DFG).

-
- ¹R. K. Crouch, J. B. Robertson, and T. E. Gilmer, Jr., *Phys. Rev. B* **5**, 3111 (1972).
- ²J. N. Heyman, A. Giesekeus, L. M. Falicov, and E. E. Haller, *Bull. Am. Phys. Soc.* **35**, 279 (1990).
- ³J. N. Heyman and E. E. Haller, *Bull. Am. Phys. Soc.* **36**, 862 (1991); J. N. Heyman, A. Giesekeus, and E. E. Haller, in *Proceedings of the 16th International Conference on Defects of Semiconductors*, edited by G. Davies, G. DeLeo, and M. Stavola (Trans Tech, Aedermannsdorf, Switzerland, in press).
- ⁴M. Kleverman and H. G. Grimmeiss, *Semicond. Sci. Technol.* **1**, 45 (1986).
- ⁵R. K. Crouch, J. B. Robertson, H. T. Morgan, T. E. Gilmer, Jr., and R. K. Franks, *J. Phys. Chem. Solids* **35**, 833 (1974).
- ⁶K. Muro and A. J. Sievers, *Phys. Rev. Lett.* **57**, 897 (1986).
- ⁷R. E. Peale, K. Muro, and A. J. Sievers, *Phys. Rev. B* **41**, 5881 (1990).
- ⁸M. O. Henry, K. G. McGuigan, M. C. do Carmo, M. H. Nazare, and E. C. Lightowers, *J. Phys. Condens. Matter* **2**, 9697 (1990).
- ⁹D. Labrie, T. Timusk, and M. L. W. Thewalt, *Phys. Rev. Lett.* **52**, 81 (1984).
- ¹⁰E. Tarnow, S. B. Zhang, K. J. Chang, and D. J. Chadi, *Phys. Rev. B* **42**, 11 252 (1990).
- ¹¹A. Giesekeus and L. M. Falicov, *Phys. Rev. B* **42**, 8975 (1990).
- ¹²A. Giesekeus and L. M. Falicov, *Phys. Rev. B* **42**, 11 725 (1990).
- ¹³E. P. Kartheuser, S. Rodriguez, and P. Fisher, *Phys. Status Solidi B* **64**, 11 (1974).
- ¹⁴M. L. W. Thewalt, D. Labrie, I. J. Booth, B. P. Clayman, E. C. Clayman, E. C. Lightowers, and E. E. Haller, *Physica B* **146**, 47 (1987).
- ¹⁵D. Labrie, I. J. Booth, M. L. W. Thewalt, and E. E. Haller, *Phys. Rev. B* **38**, 5504 (1988).
- ¹⁶E. Merk, J. Heyman, and E. E. Haller, *Solid State Commun.* **72**, 851 (1989).
- ¹⁷A. Dörnen, R. Kienle, K. Thonke, P. Stoltz, G. Pensl, D. Grünebaum, and N. A. Stolwijk, *Phys. Rev. B* **40**, 12 005 (1989).
- ¹⁸G. Davis, *Mater. Res. Soc. Symp. Proc.* **104**, 65 (1988).
- ¹⁹H. R. Chandrasekhar, P. Fisher, A. K. Ramdas, and S. Rodriguez, *Phys. Rev. B* **8**, 3836 (1973).
- ²⁰R. Baron, M. H. Young, and T. C. McGill, *Solid State Commun.* **47**, 167 (1983).
- ²¹G. D. Watkins and W. B. Fowler, *Phys. Rev. B* **16**, 4524 (1977).
- ²²R. Buczko, *Nuovo Cimento* **9**, 669 (1987).
- ²³A. A. Kaplyanskii, *Opt. Spectrosc.* **16**, 602 (1964) [*Opt. Spectrosc.* **16**, 329 (1964)].
- ²⁴M. Kleverman, J. Olajos, and H. G. Grimmeiss, *Phys. Rev. B* **37**, 2613 (1988).
- ²⁵M. S. Skolnick, L. Eaves, R. A. Stradling, J. C. Portal, and S. Askenazy, *Solid State Commun.* **15**, 1403 (1974).
- ²⁶A. Onton, P. Fisher, and A. K. Ramdas, *Phys. Rev.* **163**, 686 (1967).